

# Geometric Eye Gaze Tracking

Adam Strupczewski<sup>1</sup>, Błażej Czupryński<sup>1</sup>, Jacek Naruniec<sup>2</sup> and Kamil Mucha<sup>1</sup>

<sup>1</sup>*Samsung Electronics Poland, Warsaw, Poland*

<sup>2</sup>*Warsaw University of Technology, Warsaw, Poland*

**Keywords:** Eye Gaze Tracking, Head Pose Tracking, Iris Localization, Feature Matching, Pose Estimation.

**Abstract:** This paper presents a novel eye gaze estimation method based on calculating the gaze vector in a geometric approach. There have been many publications in the topic of eye gaze estimation, but most are related to using dedicated infra red equipment and corneal glints. The presented approach, on the other hand, assumes that only an RGB input image of the user's face is available. Furthermore, it requires no calibration but only simple one-frame initialization. In comparison to other systems presented in literature, our method has better accuracy. The presented method relies on determining the 3D location of the face and eyes in the initialization frame, tracking these locations in each consecutive frame and using this knowledge to estimating the gaze vector and point where the user is looking. The algorithm runs in real time on mobile devices.

## 1 INTRODUCTION AND RELATED WORK

Eye gaze tracking is an important aspect of computer vision as it can be applied to many purposes: enhancing human-computer interfaces (HCI), support for the disabled or user profiling are just a few. The exact spot observed by the user is the combined result of how their head is placed and how their eyes are oriented. As is mentioned in one of the most recent surveys on the topic (Hansen and Ji, 2010), the number of publications and possible approaches to tackle the problem is very large. We wanted to provide a system that would be accurate and useful to the largest possible audience - so requiring only a simple webcam to perform the gaze estimation task.

No head mounted devices meet this criterion for obvious reasons. Also, purely statistical approaches based on Markov Chains or neural networks have been rejected because of the tiresome calibration that is required and relatively low accuracy. In general, appearance-based methods report lower accuracy than model-based methods. One of the most accurate appearance-based methods (Lu et al., 2014) does report an impressive accuracy, but requires tiresome calibration for each user, and also doesn't work in real-time.

Surprisingly, the current state-of-the-art approach rather deals with the eyes only, neglecting the head motion. The two leading companies that produce

commercial eye trackers, Tobii and SensoMetric Instruments, use remote trackers with a system of infrared illuminators that produce corneal reflections on the eyeball surface and thus allow inferring the 3D cornea orientation relative to the camera. These algorithms are described for example in (Ohno et al., 2002; Hennessey et al., 2006). Besides requiring sophisticated infra red cameras, they require personal calibration to overcome the individual discrepancy between the optical axis and line of sight.

There have been many studies on using a simple webcam for eye gaze tracking. One approach is to infer the gaze direction from the elliptical shape of the observed limbus. A recent study of this performed on a tablet has been published (Wood and Bulling, 2014). Unfortunately, the reported accuracy is quite low and requires a very high resolution image of the eye, something difficult to obtain in an uncontrolled environment. Other proposed methods are mostly based on relative iris and eye corner location analysis. Ishikawa et al. (Ishikawa et al., 2004) use a geometric eye model where the gaze direction is inferred as the head pose direction and modified by the eye orientation. The eye orientation relative to the initial one is found by detecting the iris center and eye corners. While impressive results have been reported (3.2 degree accuracy under significant head movements), we have implemented a similar approach and found numerous problems. Most importantly, the AAM is in general incapable of providing accurate head pose es-

timates for different people. Additionally, the eye corners cannot be reliably detected with high accuracy in uncontrolled conditions. Moreover, when uncontrolled simultaneous head and eye movements are performed, the system produces high errors. In (Kim and Kim, 2007) a similar system is described, but the reported eye gaze tracking accuracy is only around 10 degrees.

Others (Valenti et al., 2009) propose to perform eye gaze tracking by analyzing the relative position of the pupil and the eye corners. The method is based on 9-point calibration and on interpolation of the locations from calibration during tracking. This method does not account for considerable head movements and completely ignores head rotations. Furthermore, the method strongly relies on the initial calibration and if this is inaccurate, it needs to be performed again. A significant improvement on this concept was presented in (Valenti et al., 2012). This method assumes that the head pose determines a specific field of view, whereas the eye orientations can influence which part of this field of view is observed. This way, an initial 9-point calibration with a frontal face pose can be used for any other pose as well. A cylindrical head model and optical flow are used for head pose estimation following the algorithm in (Xiao et al., 2002). Furthermore, a hybrid framework is presented where the eye center detection can be used to refine the head pose estimation by so called eye location cues, while the eye locations can in turn be refined by so called head pose cues.

The work presented in (Valenti et al., 2012) seems to be the best purely webcam based eye gaze tracking system so far, which works also under limited head movements. It has a number of drawbacks, however. Firstly, it depends on initial multiple point calibration, which is an inconvenience. Secondly, the calibration data is used for means of interpolation within the deduced field of view. This in itself limits the maximum achievable accuracy, as the point of regard does not stem from a true geometric model. Furthermore, the isophote based iris localisation and head pose estimation both leave space for improvement.

We propose a new direct geometrical method of eye gaze direction estimation. Similarly as the approach of (Valenti et al., 2012), it relies on head pose estimation and iris localization. The main concept of our method is different, however. It is based on an explicit 3D geometric model where the eye gaze is defined as a vector passing through specific points of the eye. These points are calculated to directly determine the gaze vector, without any interpolation or statistical inference. In the course of development we have also designed a highly robust and accurate

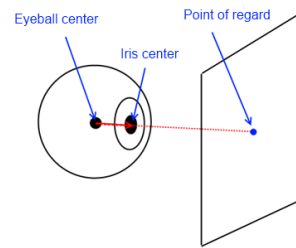


Figure 1: Eye gaze tracking method concept.

head pose estimation method, which we believe lies in the state-of-the-art category. It is an expansion of renown model-based head pose estimation methods (Xiao et al., 2002; Jang and Kanade, 2004; Morency et al., 2008; Liao et al., 2010). Finally, we have improved previously published iris localization algorithms (Zhang et al., 2007; Zhou et al., 2011) to use head pose information for adaptive tuning.

The contributions of this paper are the following:

1. A complete geometric method for eye gaze tracking which can be used without user-specific calibration; the method can use RGB only input
2. A novel hybrid method for accurate head pose estimation
3. A novel adaptive method for iris localisation
4. A framework to evaluate the accuracy of eye gaze tracking

## 2 PROPOSED METHOD

We propose a straightforward geometric method that calculates the gaze vector as a line in 3D space crossing the eye center, the pupil center and the observed screen. The intersection of this line with the screen is the point of regard (POR) on the screen. The pupil center is approximately the same point as the iris center. Therefore, we always localize the iris and use its center as the pupil center. The concept of the proposed method is shown in Figure 1.

The big benefit of this approach compared to other approaches is that its accuracy is not inherently limited by the method. If accurate pupil center and eyeball center data is measured, an accurate POR can be calculated. In contrast, most statistical approaches that interpolate between calibration measurements are unable to achieve such high accuracy.

While having many advantages, the proposed concept requires the knowledge of the pupil center and eye center locations in 3D. The only thing that can be directly measured in an image is the 2D location of the iris center. This is generally the same point as the

pupil center, and can be treated as such. This is further described in Section 2.2. The actual distance of the iris and eye center from the camera is unknown. Clearly, some other source of information is necessary to obtain the required 3D coordinates.

We have decided that requiring tedious multiple-point calibration from the user every time they want to use the system is very inconvenient. We have therefore opted to use a simple, one-point initialization scheme. It assumes that the user looks at a specified point when starting to use the system. The point is clearly displayed at the center of the screen, so it requires little effort from the user. If the POR and iris location are both known, the gaze vector can be estimated. This gaze vector unambiguously determines the eyeball center, given a known eye radius. Luckily, the eye radius is relatively invariable for most people and is very close to 12mm (Riordan-Eva et al., 2004). Furthermore, the eye reaches its full size for children at the age of 13. This means that a system based on the assumption that the eye radius is 12mm will work well for a great majority of the population. Those people who have an unusual eye size will experience slightly less accurate functioning of the eye gaze tracking algorithm, but the deterioration will be gradual and the system will never fail completely. A method to eliminate the eye size inaccuracies completely is described in Section 2.4.

The second important unknown variable is the head distance from the camera along the z axis. In order to calculate this accurately, it is sufficient to know the camera parameters and real distance between the eyes. In a pinhole camera model the perspective projection formula for a 3D point  $P$  and its location  $p$  in the camera image is:

$$\begin{bmatrix} p_x \\ p_y \end{bmatrix} = \frac{f}{F_z} \begin{bmatrix} P_x \\ P_y \end{bmatrix} \quad (1)$$

assuming that  $f$  is the focal length of the camera which is the same in the horizontal and vertical planes. From (1) we derive the z distance of the face from the camera:

$$P_z = f \frac{P_{x1} - P_{x2}}{p_{x1} - p_{x2}} \quad (2)$$

The distance between the eyes in pixels,  $p_{x1} - p_{x2}$ , can be measured from the input image. The real distance between the user's eyes,  $P_{x1} - P_{x2}$ , can be approximated as 6cm (Dodgson, 2004) or measured manually and configured individually. Throughout our experiments we have used the true distance between the eyes measured for each person with a ruler. Except for measuring the distance between the eyes with a ruler, it can also be calibrated automatically as described in Section 2.4. It should be noted that the head distance

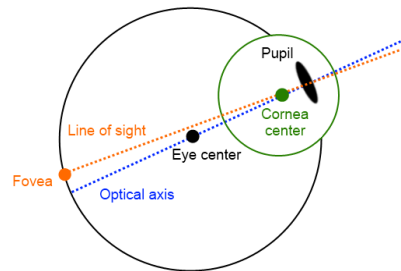


Figure 2: Optical axis vs line of sight.

measured by this method actually refers to the iris distance from the camera - as the iris centers are used for calculations. This is as good a measurement as any, because the face has different depths at different places and any of them can be used for determining head distance. A benefit of using irises is that the exact 3D locations of the irises can then be calculated. Combining this information with the gaze vector and eye radius allows to accurately determine the eyeball centers.

Here it should be noted that the visual axis and line of sight are in principle two different things, as shown in Figure 2. Eye gaze tracking systems can only measure the optical axis, whereas the actual eye gaze of a person is determined by their line of sight. It has been reported, that the discrepancy can be as much as 5 degrees (Goss and West, 2002). IR based approaches require user specific calibration to overcome this. In our method the initialization phase accounts for this difference. The calculated eye center is not the true geometrical eye center, but a central point lying on the visual axis. Therefore, each eye gaze measurement based on this initial model will inherently account for the angle between the optical axis and line of sight. Head movements will cause certain inaccuracies as a different point than the true optical center will be tracked, but these will be significant only for very large head movements.

As has been shown, using two simple assumptions, the iris centers and eyeball centers can be determined in the initialization frame. In order for eye gaze tracking to work, not only the iris needs to be found in each consecutive frame, but the eye center locations also need to be calculated. This can be achieved through head pose tracking, as the relative eye and face position does not change over time. Accurate head pose estimation is crucial for performing geometric eye gaze tracking in this fashion.

## 2.1 Head Pose Estimation

As mentioned in (Czuprynski and Strupczewski, 2014), the most accurate head pose tracking methods

are based on tracking. Despite the high accuracy of these methods, they are vulnerable to drift and getting completely lost if tracking gets lost. This in turn would cause the entire eye gaze tracking system to fail. Therefore, a hybrid combination of tracking and detection is the optimal solution. When tracking fails, redetection is performed and the head pose tracking system recovers also removing the accumulated drift error in the process.

To begin with head pose tracking, and also iris localisation, an approximate face position is required. Purely detection based methods such as (Viola and Jones, 2004) have been found to provide insufficient accuracy. Eventually, an Active Appearance Model (AAM) based approach was chosen. AAMs begin with a coarse face position and iteratively optimize the alignment of a model to fit the query image (Cootes et al., 2001). More recently, more robust and efficient implementations have been proposed (Matthews and Baker, 2004; Xiao et al., 2004). We have used a proprietary implementation of these algorithms in our eye gaze tracking system. Due to its high efficiency, it can be run as a background supporting process to the whole eye gaze tracking system.

The AAM allows to determine the relevant face contour, the main facial features (eyes, nose, lips) and an estimate of the face scale and rotations. This is crucial information for initializing the tracking algorithm. We perform initialization by fitting a generic mesh to the user's face and later track it using optical flow or feature matching. Initially, a cylindrical head model similar to that in (Xiao et al., 2002) was used. Later experiments have however shown that a more precise face model allows more accurate tracking. Eventually, a generic facial shape was created by recording 10 users with Kinect and averaging their faces. It is shown in Figure 3. This person-like mesh has demonstrated far superior performance compared to using a cylindrical model. In general, as stated in (Morency et al., 2008), a more accurate model that better fits the user's real face allows for more accurate tracking, but also fails more quickly when drift accumulates. Following this reasoning, we have modified the algorithm further to use the AAM points for warping the generic model to the specific user's face. This has allowed to achieve even bigger improvement in head pose tracking accuracy.

While a very well fitted model to the face is desired, it is highly prone to drift errors. For instance, the cylindrical model still works with roughly the same accuracy if it drifts by three degrees of horizontal rotation (the model still has the same fit quality to the face), whereas the finely personalized model tends to fail completely for similar discrepancies (the nose,

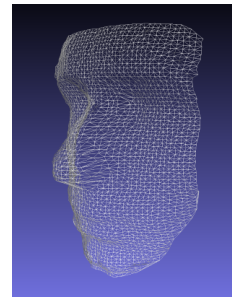


Figure 3: Generic face mesh.

eyes etc. all get dislocated). This high sensitivity to drift error was the main driving factor to consider a hybrid head pose tracking approach. In our method we use a combination of the methods presented in (Xiao et al., 2002; Jang and Kanade, 2004; Morency et al., 2008; Liao et al., 2010), as described in the following sections.

### 2.1.1 Optical Flow Tracking

Our implementation of the optical flow model-based head pose tracking algorithm closely follows the description in (Xiao et al., 2002). We use a mesh of evenly distributed points, but having a personalized shape instead of the shape of a cylinder. This method works directly on image luminance. Each point of the mesh is tracked in 2D using optical flow and all computed point translations contribute to a rigid 6D model transformation (3 translations and 3 rotations). For this and further derivations it will be useful to introduce some of the used notation.

Throughout this paper we use a simple pinhole camera model where the projection is in accordance with formula (1). Let us represent the head pose change between frames relative to the camera as a motion vector in the twist representation:

$$\mu = [t_x, t_y, t_z, \omega_x, \omega_y, \omega_z] \quad (3)$$

Where  $t_x, t_y, t_z$  denote translations relative to the camera and  $\omega_x, \omega_y, \omega_z$  denote rotations relative to the camera. From rigid body motion theory we get that the 3D point position at time  $t$  is given by:

$$P_t = M \cdot P_{t-1} \quad (4)$$

Where  $M$  is a transformation matrix based on  $\mu$ :

$$M = \begin{bmatrix} 1 & -\omega_z & \omega_y & t_x \\ \omega_z & 1 & -\omega_x & t_y \\ -\omega_y & \omega_x & 1 & t_z \\ 0 & 0 & 0 & 1 \end{bmatrix} \quad (5)$$

Given the transformation matrix  $M$ , the projection of  $P_t$  can be expressed using the previous position  $P_{t-1}$  and motion parametrized by vector  $\mu$ :

$$p_t = \frac{\begin{bmatrix} X_t \\ Y_t \end{bmatrix} \cdot f}{Z_t} = \frac{\begin{bmatrix} X_{t-1} - Y_{t-1}\omega_z + Z_{t-1}\omega_y + t_x \\ X_{t-1}\omega_y + Y_{t-1}\omega_x - Z_{t-1}\omega_x + t_y \\ -X_{t-1}\omega_y + Y_{t-1}\omega_x + Z_{t-1} + t_z \end{bmatrix} \cdot f}{-X_{t-1}\omega_y + Y_{t-1}\omega_x + Z_{t-1} + t_z} \quad (6)$$

Let the intensity of the image at point  $p$  and time  $t$  be denoted as  $I(p, t)$ . Let  $F(p, \mu)$  be a function that maps point  $p$  into a new location  $p'$  using vector  $\mu$ , according to the motion model given by (6). Let the region containing all considered face pixels be denoted as  $\Omega$ . Computing the motion vector between two frames based on luminance can be expressed as the minimization of the sum of luminance differences between the face image from previous frames and the current face image transformed by the mapping function  $F$ :

$$\min \left( \sum_{p \in \Omega} (I(F(p, \mu), t) - I(p, t-1))^2 \right) \quad (7)$$

Following the original derivation in (Xiao et al., 2002), we compute the motion vector  $\mu$  using the Lucas-Kanade method:

$$\mu = \left( \sum_{\Omega} w (I_p F_{\mu})^T (I_p F_{\mu}) \right)^{-1} \sum_{\Omega} w (I_t (I_p F_{\mu})^T) \quad (8)$$

Where  $I_t$  and  $I_p$  are temporal and spatial image gradients, while  $w$  is a weight assigned to each point.  $F_{\mu}$  denotes the partial differential of  $F$  with respect to  $\mu$  at  $\mu = 0$ :

$$F_{\mu} = \begin{bmatrix} -XY & X^2 + Z^2 & -YZ & Z & 0 & -X \\ -(Y^2 + Z^2) & XY & XZ & 0 & Z & -Z \end{bmatrix} \frac{f}{Z^2} \quad (9)$$

We compute motion iteratively. After each iteration, the model is transformed using the computed motion vector and the weights for all points are updated. Furthermore, to handle large movements without loss of accuracy, tracking is performed on a gaussian image pyramid. In the original article each mesh point was weighted by a combination of three weights depending on the strength of the image gradient, the density of the projected model points and the luminance difference before and after the model transformation. In our experiments we have found that the first two do not improve tracking accuracy in a consistent manner. Therefore, we only use the third weighting method, which decreases the impact of points which are not consistent with the estimated model motion in an exponential fashion. This reduces the impact of inaccurate alignment of the model, non-rigid motion, illumination changes or occlusions.

We think that the presented tracking method works better than the original mostly because of better initialization and mesh alignment. These factors

are absolutely crucial for model-based tracking accuracy. Another important difference is the reinitialization method. Originally, it was proposed to save a luminance template of the first frame and for every frame attempt to track to this template frame - if this is successful reinitialization is performed. In practice this reinitialization method is not stable and often introduces large random errors. We have decided to abandon this completely in favour of a much more accurate and efficient reinitialization procedure. This is described in Section 2.1.3.

## 2.1.2 Feature Tracking to Template

Optical flow is one way to determine correspondences between frames. Another, conceptually different way is by matching feature points. Since the publication of SIFTs (Lowe, 2004), feature points have been used extensively in many areas of computer vision. In fact, several interesting experiments using feature points for head pose estimation have been published, improving the work of (Vacchetti et al., 2004). For instance, (Jang and Kanade, 2004) propose to use features for cylinder model based head pose estimation in a framework where motion is estimated based on matched SIFT points. The motion was estimated between consecutive frames and to a set of stored keyframes, integrated with the Kalman filter. More recently, (Liao et al., 2010) propose to use intensity based tracking (optical flow) and feature based tracking simultaneously and weight them according to the tracking error. We have implemented continuous feature based pose estimation and found that it is very prone to drift - in fact much more than optical flow methods. On the other hand, features can be detected independently in each frame, which means that there is no drift error in the matched features themselves. This is an important advantage when considering the reinitialization concept. Eventually, it turned out that feature based head pose estimation is the ideal method for tracking to template frames (keyframes) for reinitialization purposes.

Let us introduce the concept of pose estimation based on local features. Let us assume that two independent sets of feature points are detected in two facial images. Let us assume further that a subset of these points was matched to form pairs  $(p_{t-1}, p_t)$ . The points from the first frame are related to a known head pose, so their 3D coordinates,  $P_{t-1}$ , are known. Therefore, two forms of point coordinates in the second image are available. The first are the observed locations of the detected points  $p_t$ . The second form are the projections  $p'_t$  of the points  $P_{t-1}$ , obtained by estimating the motion of the previous locations  $P_{t-1}$  based on the 3D model and motion vector  $\mu$ . Assum-

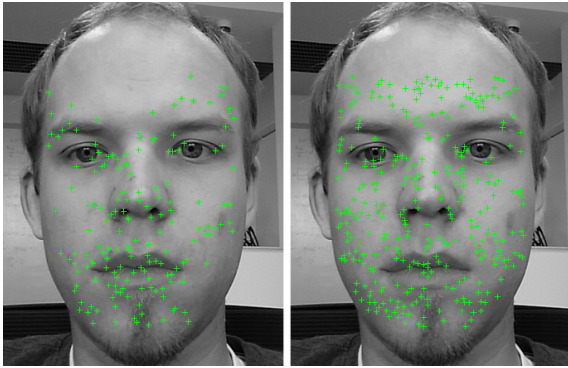


Figure 4: Left image shows SIFT features, right image shows STAR features.

ing  $N$  such point pairs have been collected, the goal is to compute motion vector  $\mu$ , which minimizes the sum of distances between the observed points  $p_{i,t}$  and the estimated points  $p'_{i,t}$ . It can be achieved by solving the following equation set using the linear least squares method:

$$\begin{cases} |p_{0,t} - p'_{0,t}| = 0 \\ \vdots \\ |p_{N,t} - p'_{N,t}| = 0 \end{cases} \quad (10)$$

Where the estimated points are given by:

$$p'_{i,t} = [P'_{i,t}]_{PROJ} = [M \cdot P_{i,t-1}]_{PROJ} \quad (11)$$

Although first results of the above algorithm were promising, we have found that SIFT points are not ideally suited for usage with faces. Faces contain few corner points and are unlike the typical scenes that SIFT points were designed for. After testing various point detectors we have found that the best results are achieved when using the STAR feature detector with a low detection threshold. A comparison of SIFT and STAR detectors is shown in Figure 4.

As the feature descriptor we have decided to use BRISK (Leutenegger et al., 2011). This is because it is lightweight, robust and free to use. The accuracy of the final feature based head pose tracking algorithm was above expectations. All head poses within the range of at least 10 degrees from a frontal pose could be correctly estimated using a single template. For small rotations it was impossible to visually observe any inaccuracy when analysing the mesh. This is shown in Figure 5.

### 2.1.3 Hybrid Algorithm

The work of (Morency et al., 2008) proposes to combine differential tracking, keyframe tracking and static pose estimation using the Kalman filter. The

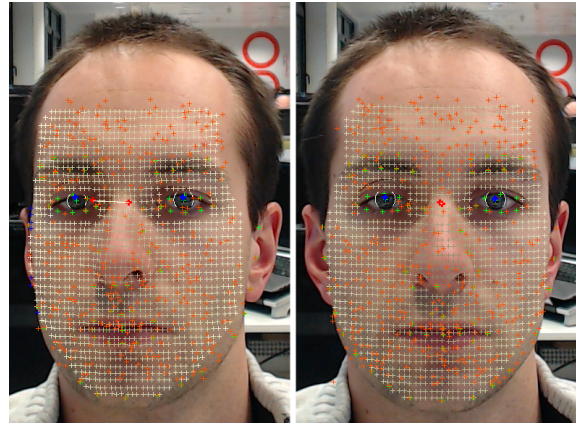


Figure 5: Feature tracking to single frontal template.

Kalman filter is also used in (Jang and Kanade, 2004). Each of these algorithms relies on multiple keyframes, which are collected while the algorithm is running. This contributes to a nice visual effect, but unfortunately deteriorates tracking accuracy. Any form of collecting templates with drift is bound to increase the overall tracking error, despite improving the robustness of the system. This can be seen if one looks closely at the videos available at Takeo Kanade's website (Jang and Kanade, 2010).

In the use case of eye gaze tracking we have evaluated two approaches:

- Online collecting of multiple separate templates with features for various head poses
- Online growing of a single template with features from many frames, with feature points aligned to form a single 3D model

In the first case each template that was collected while the system was running contained a certain drift. Unfortunately for the eye gaze tracking scenario, using a template with drift has negative consequences. All in all, this approach has worsened the eye gaze tracking algorithm accuracy, especially in case of large head movements. The improvement in robustness does not compensate sufficiently for the deterioration.

In the second case the idea was to combine the 3D mesh warped during initialization with new features detected in later frames. This can be important as when the user rotates their head, different feature points become visible than in the frontal pose. Thus, a single composite model can be formed with all points aligned according to how the 3D model was tracked over time. In principle this approach suffers from the same drift error as the previous one, except the drift error is only associated with the additional features added to the composite model. If very accurate tracking is performed, the drift error can be very small and

the additional points collected over time improve the robustness of the system (there are more points than in the case of a single template). However, if the points are added during less accurate tracking, they have a negative impact. In practice, we have found that when only points from a frontal pose are added to the model, when very little or no head movement has been made since initialization, it improves the tracking system. Because the camera sensor is noisy, even frames with exactly the same pose can contain up to 25% different feature points.

The second described strategy can sometimes significantly improve tracking robustness, although it is highly dependant on the initialization and the shape of the user's face. Nonetheless, as the most accurate method available, it has been chosen as the basic tracking mode. We have found a good strategy to be growing an aggregate template using 5 to 10 initial frames. After this, feature and optical flow model-based tracking are performed simultaneously for each new frame. The tracking method that gives smaller error is chosen. Typically, for poses very close to the initial pose feature tracking will outperform optical flow tracking, whereas for other poses, when few features can be matched to the initial template, optical flow will provide much better accuracy. When one of the methods gives a very large error compared to the other one, it is simply discarded. The error is calculated as the luminance difference between the mesh points before and after the transformation.

One more thing that should be mentioned here is usage of the AAM. It is a third algorithm running virtually all the time. Its main role is guidance in the case of reinitialization - when all other tracking fails. Reinitialization can be performed by using the face location based on the AAM output and calculating feature points. These feature points are then matched to those of the stored face template. Once the relative pose to the stored template is known, the 3D mesh can be reinitialized and tracked using the hybrid tracking algorithm described above.

## 2.2 Iris Localisation

We use eye regions extracted by the AAM algorithm to search for the iris. We have found that the best iris detection accuracy is achieved in a dual approach consisting of two stages. The first stage aims to perform coarse localisation and is based on the Hough transform. The second stage provides a refinement based on Circular Integro Differential Operator. Our approach is partly similar to (Zhou et al., 2011). Each stage will be described in the following sections.

### 2.2.1 Coarse Iris Localization

Coarse iris estimation is based on a voting technique. The approach is very similar to the Circle Hough Transform (CHT). It is based on the assumption, that the iris bound is a transition between a bright outside region and a dark inside region of the iris. The exact radius of the eye is unknown, but its potential range can be estimated based on the face size in pixels. Only right and left iris boundary pixels are considered, because the upper and lower bounds can be occluded by the skin around the eye. As a result, assuming that the face is upright, only edges that have a vertical direction (first order derivative angle direction is larger than 45 degrees) are considered.

The algorithm works as follows. First, the relevant image region is prepared and first order derivatives are computed for each pixel. Every pixel is analysed and if the gradient is strong enough and vertical enough, it votes for the iris center according to the gradient direction and currently analysed radiuses. Several passes of the algorithm are completed for various radii. The voting bins are later blurred by a Gaussian kernel and the maximum among pixel locations and radii is chosen as the rough iris center position. To provide additional robustness, we weight the voted centers with the inverse of the region's brightness. This favours dark regions, such as the pupil should be, and helps to prevent misdetections.

### 2.2.2 Fine Iris Localization

Fine localization of the eye center is based on Daugman's integro-differential operator. Similarly as in the original publication (Daugman, 2002), a set of ellipses is matched with the iris contour in order to maximize the sum of Daugman's circular integro-differential operator:

$$\max_{(r, x_c, y_c)} \left| G_\sigma(r) \star \frac{\partial}{\partial r} \int_{r, x_c, y_c} \frac{I(x, y)}{2\pi r} ds \right| \quad (12)$$

Where  $I(x, y)$  is the gray level of the image and  $G_\sigma(r)$  is the Gaussian smoothing filter. The operator searches over the iris image domain  $(x, y)$  for the maximum change in pixel values, with respect to increasing radius  $r$  along a circular  $ds$  of radius  $r$  and center coordinates  $(x_c, y_c)$ . To achieve a speed up, the algorithm is performed in a coarse to fine fashion - the used  $\Delta r, \Delta x, \Delta y$  are larger in the first stage, and smaller in later stages. Altogether three stages are used, which provides optimum efficiency with the desired accuracy.

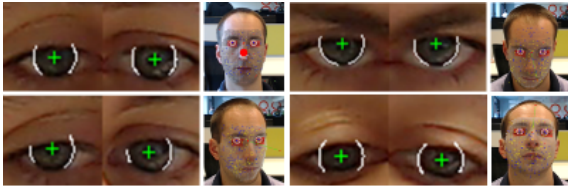


Figure 6: Adaptive iris localisation.

### 2.2.3 Adaptive Behaviour

In order to reduce the influence of eyelids, eyelashes and other skin parts we only consider vertical parts of the iris when calculating the radial sum in equation (12). However, this is not accurate enough, as depending on the person and where they are looking, different parts of the iris are visible. Therefore, we ignore a certain percentage of the gradient lying on the circle depending on gradient strength. Thus, only a subset of the vertical gradients is used for calculations. What is more, an analysis of the relation between the looking direction and visible iris contours has shown that the correlation is very strong. We have therefore developed an adaptive version which considers the eye gaze and head pose of the person in order to optimally select which parts of the iris should be used for calculations. Figure 6 shows which parts of the iris are chosen for refinement depending on the eye rotation relative to the head.

We propose to use the following methodology. Traditionally, only vertical iris boundaries are considered - this means half of all the points. To determine which points to use, a top and bottom boundary threshold can be established. Furthermore, the left and right side of the iris can require different treatment, as is shown in Figure 6. Therefore, for each side of the iris, left and right iris boundary thresholds can be established. This gives altogether four angular thresholds: left top, left bottom, right top and right bottom. We propose to adjust these thresholds according to head rotations and gaze directions, as follows:

$$\begin{cases} \theta_{lt} = \theta_{lt} (1 + \alpha_l \cdot (gx - rx) + \beta_l \cdot (gy - ry)) \\ \theta_{lb} = \theta_{lb} (1 + \alpha_l \cdot (gx - rx) + \beta_b \cdot (gy - ry)) \\ \theta_{rt} = \theta_{rt} (1 + \alpha_r \cdot (gx - rx) + \beta_l \cdot (gy - ry)) \\ \theta_{rb} = \theta_{rb} (1 + \alpha_r \cdot (gx - rx) + \beta_b \cdot (gy - ry)) \end{cases} \quad (13)$$

Where  $rx, ry$  are head rotations and  $gx, gy$  are gaze angles in the horizontal and vertical planes. The parameter values of  $\alpha_l, \alpha_r, \beta_l, \beta_b$  have been chosen experimentally based on the available test sequences.

An evaluation of the described algorithm was performed on a manually tagged set of webcam images and is described in section 3.

## 2.3 Mutual Head Pose and Iris Relation

In our eye gaze tracking system the iris positions are used to refine the head pose estimation. This is done during initialization. As was mentioned in Section 2.1, the head distance from the camera along the z axis has to be estimated in the first frame. For this, the distance between the eyes is used, and this can be most accurately measured as the distance between the irises. What is more, the irises are used as reference points for aligning and warping the mesh during initialization. No facial feature can be detected as accurately as the irises, so this strategy is the best. A better aligned mesh at the beginning of tracking leads to better results.

At the same time, the head pose is used to refine iris localisation. First of all, the head pose determines the regions which are used for iris searches. The regions can be determined by AAM points, or taken from the mesh directly if the AAM is not used in every frame. Secondly, once the eye gaze vector is known, it is the head pose that determines which parts of the iris contours are visible in the image. This information is used directly in the adaptive refinement stage as described in Section 2.2.3.

## 2.4 Calibrating Eye Depth and Head Size

It has earlier been mentioned that the proposed system makes the assumption of a typical eye radius (12mm) and face size (6cm between irises) for each person unless configured otherwise. While the distance between the eyes can be quite easily measured manually by the user with a ruler, the eye radius, and so eye center depth relative to the iris, is impossible to measure explicitly. Both of these unknown values can be measured automatically. Let us assume that the user is looking at a known point in several different frames and moves their head. Let us assume further, that the head pose can be tracked with at least basic accuracy, based on the generic face size assumption and mesh tracking as described in Section 2.1.1. In all those frames, the irises are detected, and the gaze point is known. Therefore, the gaze vector is known. What remains unknown is the eye center location. But, for each frame it has to lie somewhere along the gaze vector. If the head pose transformation is known from the head pose tracking algorithm, a set of equations can be formed to find this unknown eye depth:

$$\begin{cases} M_0 \cdot P_{eye} = \lambda \cdot \vec{g}_0 \\ \vdots \\ M_n \cdot P_{eye} = \lambda \cdot \vec{g}_n \end{cases} \quad (14)$$

Where  $M_t$  is the current estimation of the head pose,  $P_{eye}$  is the 3D eye center position in head-relative coordinates,  $\vec{g}_t$  is the gaze vector and  $\lambda$  is a scaling factor that stretches a unit gaze vector from the camera to the eye center. The above applies to the situation when the user is looking straight at the camera. For other gaze points the formulas get more complicated, but the concept remains the same.

As the eye location is the same in head-relative coordinates, the gaze vectors and head pose transformations are the only variables that change. The scaling factor  $\lambda$  only depends on the face distance from the camera, and so its relative change is also assumed to be known from head pose tracking. This means that a set of at least two equations allows to find the true 3D eye location along with the scaling factor  $\lambda$ . In practice, at least several measurements should be used to reduce the measurement error. If many measurements are available, one may assume that the z distance in M is unknown, and calculate it together with the relative eye depth. Thus, the face size can be established without the need to measure it with a ruler.

In practice, the described calibration method works well only when the calibration data is of high quality. As the calibration depends on the user and lighting conditions, we have opted to leave this as an option and not use it as an integral part of our system.

### 3 EXPERIMENTS

We have performed multiple evaluations of the eye gaze tracking components - head pose tracking and iris tracking. We believe that both presented head pose tracking and iris tracking algorithms are in the state-of-the-art category. To remain concise, we present only the measured accuracy of the whole eye gaze tracking system.

#### 3.1 Test Framework

To evaluate the performance of the developed algorithms we have created a dedicated, novel test framework. It works on recorded test sequences and is able to measure the difference between the real place where the user is looking and the estimation given by the system. The test sequences are recorded by displaying a point on the screen and asking the user to look at it. We propose to use two stages: one with a motionless head and one with head movements. This allows to identify the weaknesses of the algorithm easier. During the phase without head movements, the marker is shown in the center of the screen during initialization and moves near the four screen corners,

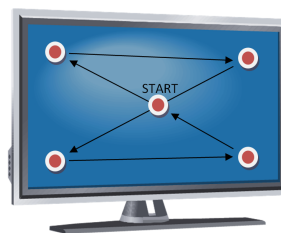


Figure 7: Locations where the user has to look during a test sequence.

but leaving a margin of 7.5% of the screen width and height from the exact corners. During the phase with head movements, the marker is placed in the screen center, so the system measures simply how robust the algorithm is in terms of head movement compensation. Figure 7 shows exactly how the test points were shown on the screen and in which order.

When the test point was moving between the five states on the screen, the gaze calculation error was not measured. Thus, any inaccuracy resulting from delays was not considered.

In order to evaluate the system, we have prepared 10 test sequences with different people using a simple 1080p webcam. Each sequence was recorded for 15 seconds at a 15 fps frame rate. This means that each test sequence consists of around 225 frames. Figure 8 shows what kind of head movements were performed.

Additionally to measuring the point of regard of the user, the head pose tracking accuracy and iris tracking accuracy can be compared with manually tagged ground truth. We have developed a tagging application that allows to tag the iris centers, inner and outer eye corners and lip corners. This can be tagged for every frame. When tracking and iris localisation is performed, the facial features tagged in the first frame and consecutive frames can be compared and any discrepancies measured. Of course, if ideal tracking was performed, the tracked features from the first frame would coincide with tagged features in other frames. We have been able to measure average errors of tagged facial features less than one pixel, but such measurements do not say much as the manual tagging is of limited accuracy. It is slightly easier to tag the iris, especially with our radial fitting tool, that allows to place a circle of variable size over the magnified iris image. We have measured an average iris detection error below 0.85 pixel for low-quality image sequences having 100 pixels between the eyes, and an average error below 0.7 pixel for high quality image sequences having 150 pixels between the eyes. Figure 9 shows these results obtained from tagged test sequences.

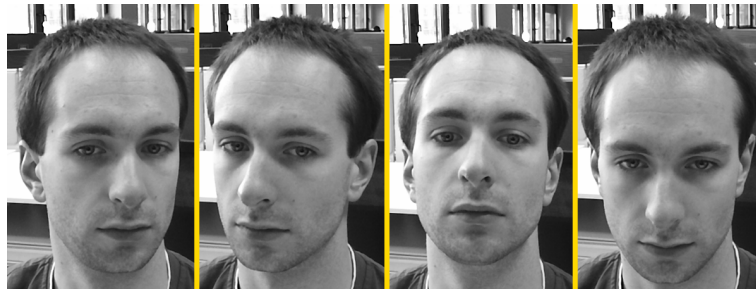


Figure 8: Illustration of head movements performed during test recording.

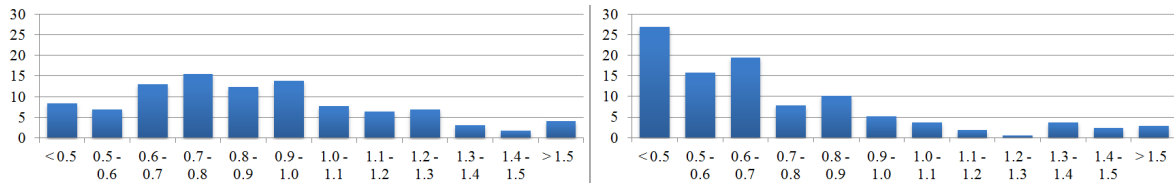


Figure 9: Percentage of iris images localized with an error within given pixel range. Left: Low quality data. Right: High quality data.

Table 1: Webcam eye gaze tracking results for hybrid mode [degrees].

Stage	Seq1	Seq2	Seq3	Seq4	Seq5	Seq6	Seq7	Seq8	Seq9	Seq10	Average
<b>1</b>	0.91	0.74	1.06	2.32	2.95	2.79	3.09	1.80	1.78	0.87	1.67
<b>2</b>	1.78	1.82	5.51	2.62	2.31	2.88	1.45	1.56	3.20	3.48	2.42
<b>total</b>	1.30	1.24	3.45	2.48	2.68	2.83	2.27	1.67	2.50	2.05	2.25

### 3.2 Test Results

The test results for the optimal hybrid head pose tracking mode with aggregate template usage and adaptive iris localisation as described in Section 2.2.3 are shown in Table 1. We have measured the angular errors between ground truth and measured gaze directions. In the test sequences, the user was seated around 70cm away from the display. The display that we used is 51cm wide.

As can be noticed in Table 1, the results for the second phase when the head is moving are significantly worse. This is quite understandable, as during the first phase virtually no head movement analysis is required. Furthermore, it is clear that the results are significantly different for each sequence. This suggests that the generic mesh has different alignment

errors for each user despite user specific warping at initialization. Perhaps an even more accurate initialization procedure could help, such as usage of a depth camera. Another possible reason for the discrepancies among results are the iris characteristics causing different behaviour of the iris detection algorithm for each person. We have noticed a high sensitivity of to this algorithm to user appearance, especially in the vertical plane.

Apart from the best achieved results, we would like to present the improvement achieved when using hybrid head pose tracking compared to using a single tracking method. Figure 10 compares the mean absolute errors between the different tracking configurations.

The hybrid method is clearly better than any single tracking method. A further interesting observation is that the aggregate template mode is slightly less accurate than the corresponding mode with a single template (larger error in stage one), but much more robust to head movements (smaller error in stage two). All the measured errors result from two factors: A slightly inaccurate eye model (which is person specific) and inaccuracies in tracking the eyeball center with the head - so in fact inaccuracies of head pose tracking.

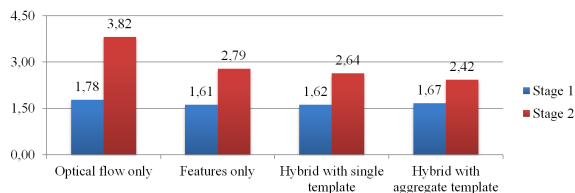


Figure 10: Eye gaze tracking algorithm accuracy comparison - POR error [degrees].

In comparison to other leading researches on the topic of webcam eye gaze tracking (Ishikawa et al., 2004; Kim and Kim, 2007; Valenti et al., 2012), we have demonstrated that our system achieves better accuracy. An average error of 2.25 degrees measured with significant head movements is better than other systems reporting an accuracy between 3 and 5 degrees.

## 4 CONCLUSIONS

We have presented a novel eye gaze tracking method that requires only webcam quality RGB images. We have demonstrated that this method performs favourably to other systems presented in literature. We believe that extending the idea further with more accurate sensor readings, such as a depth sensor, can lead to an even more accurate eye gaze tracking algorithm which will be used in commercial systems in the near future.

A further advantage of our approach is its capability to run in real time on contemporary mobile devices. We have ported the algorithm to the Galaxy S4 smartphone and were able to obtain a speed of 15 fps at a camera resolution of 640x480 pixels, when the user was approximately 40cm away from the smartphone.

## REFERENCES

- Cootes, T. F., Edwards, G. J., and Taylor, C. J. (2001). Active appearance models. *IEEE Trans. Pattern Anal. Mach. Intell.*, 23(6):681–685.
- Czuprynski, B. and Strupczewski, A. (2014). High accuracy head pose tracking survey. In *Active Media Technology*, volume 8610 of *Lecture Notes in Computer Science*, pages 407–420. Springer International Publishing.
- Daugman, J. (2002). How iris recognition works. *IEEE Transactions on Circuits and Systems for Video Technology*, 14:21–30.
- Dodgson, N. A. (2004). Variation and extrema of human interpupillary distance.
- Goss, D. A. and West, R. (2002). *Introduction to the optics of the eye*. Butterworth-Heinemann.
- Hansen, D. W. and Ji, Q. (2010). In the eye of the beholder: A survey of models for eyes and gaze. *IEEE Trans. Pattern Anal. Mach. Intell.*, 32(3):478–500.
- Hennessey, C., Noureddin, B., and Lawrence, P. (2006). A single camera eye-gaze tracking system with free head motion. pages 87–94.
- Ishikawa, T., Baker, S., Matthews, I., and Kanade, T. (2004). Passive Driver Gaze Tracking with Active Appearance Models. Technical Report CMU-RI-TR-04-08, Robotics Institute, Carnegie Mellon University, Pittsburgh, PA.
- Jang, J. and Kanade, T. (2004). Robust 3d head tracking by online feature registration.
- Jang, J.-S. and Kanade, T. (2010). Robust 3d head tracking by view-based feature point registration. Available at [www.consortium.ri.cmu.edu/projCylTrack.php](http://www.consortium.ri.cmu.edu/projCylTrack.php).
- Kim, J.-T. and Kim, D. (2007). Gaze Tracking with Active Appearance Models. Technical report, Department of Computer Science and Engineering, Pohang University of Science and Technology.
- Leutenegger, S., Chli, M., and Siegwart, R. Y. (2011). Brisk: Binary robust invariant scalable keypoints. In *Proceedings of the 2011 International Conference on Computer Vision, ICCV '11*, pages 2548–2555, Washington, DC, USA. IEEE Computer Society.
- Liao, W.-K., Fidaleo, D., and Medioni, G. (2010). Robust: Real-time 3d face tracking from a monocular view. *J. Image Video Process.*, 2010:5:1–5:15.
- Lowe, D. G. (2004). Distinctive image features from scale-invariant keypoints. *Int. J. Comput. Vision*, 60(2):91–110.
- Lu, F., Okabe, T., Sugano, Y., and Sato, Y. (2014). Learning gaze biases with head motion for head pose-free gaze estimation. *Image and Vision Computing*, 32(3):169–179.
- Matthews, I. and Baker, S. (2004). Active appearance models revisited. *Int. J. Comput. Vision*, 60(2):135–164.
- Morency, L., Whitehill, J., and Movellan, J. (2008). Generalized adaptive view-based appearance model: Integrated framework for monocular head pose estimation. pages 1–8.
- Ohno, T., Mukawa, N., and Yoshikawa, A. (2002). Freegaze: A gaze tracking system for everyday gaze interaction. pages 125–132.
- Riordan-Eva, P., Whitcher, J., Vaughan, D., and Asbury, T. (2004). *Vaughan & Asbury's General Ophthalmology*. A Lange medical book. Lange Medical Books/McGraw Hill Medical Pub. Division.
- Vacchetti, L., Lepetit, V., and Fua, P. (2004). Stable real-time 3d tracking using online and offline information. *Pattern Analysis and Machine Intelligence, IEEE Transactions on*, 26(10):1385–1391.
- Valenti, R., Sebe, N., and Gevers, T. (2012). Combining head pose and eye location information for gaze estimation. *Image Processing, IEEE Transactions on*, 21(2):802–815.
- Valenti, R., Staiano, J., Sebe, N., and Gevers, T. (2009). Webcam-based visual gaze estimation. In Foggia, P., Sansone, C., and Vento, M., editors, *Image Analysis and Processing - ICIAP 2009*, volume 5716 of *Lecture Notes in Computer Science*, pages 662–671. Springer Berlin Heidelberg.
- Viola, P. and Jones, M. J. (2004). Robust real-time face detection. *Int. J. Comput. Vision*, 57(2):137–154.
- Wood, E. and Bulling, A. (2014). Eytat: Model-based gaze estimation on unmodified tablet computers. In *Proceedings of the Symposium on Eye Tracking Research and Applications, ETRA '14*, pages 207–210, New York, NY, USA. ACM.

- Xiao, J., Baker, S., Matthews, I., and Kanade, T. (2004). Real-time combined 2d+3d active appearance models. pages 535–542.
- Xiao, J., Kanade, T., and Cohn, J. F. (2002). Robust full-motion recovery of head by dynamic templates and re-registration techniques.
- Zhang, W., Li, B., Ye, X., and Zhuang, Z. (2007). A robust algorithm for iris localization based on radial symmetry. pages 324–327.
- Zhou, Z., Yao, P., Zhuang, Z., and Li, J. (2011). A robust algorithm for iris localization based on radial symmetry and circular integro differential operator. pages 1742–1745.

